IOPscience iopscience.iop.org

Home Search Collections Journals About Contact us My IOPscience

Computer modeling of diffusion in Ni-rich Ni_3Al and composition dependence of diffusion in γ' Ni_3Al

This article has been downloaded from IOPscience. Please scroll down to see the full text article.

2008 J. Phys.: Condens. Matter 20 195221

(http://iopscience.iop.org/0953-8984/20/19/195221)

View the table of contents for this issue, or go to the journal homepage for more

Download details:
IP Address: 129.252.86.83
The article was downloaded on 29/05/2010 at 12:00

Please note that terms and conditions apply.

IOP PUBLISHING JOURNAL OF PHYSICS: CONDENSED MATTER

J. Phys.: Condens. Matter **20** (2008) 195221 (7pp) doi:10.1088/0953-8984/20/19/195221

Computer modeling of diffusion in Ni-rich Ni_3Al and composition dependence of diffusion in γ' Ni_3Al

Jinsong Duan[1]

Department of Materials Science and Engineering, Faculty of Engineering, The University of Liverpool, Liverpool L69 3GH, UK

E-mail: chemcpu@yahoo.com

Received 26 September 2007, in final form 3 March 2008
Published 17 April 2008
Online at stacks.iop.org/JPhysCM/20/195221

Abstract

Atomistic simulations of diffusion in off-stoichiometric Ni-rich Ni_3Al ($Ni_{77}Al_{23}$) at temperatures ranging from 1300 to 1550 K and comprehensive analysis of the composition dependence of Ni and Al diffusion in γ' Ni_3Al of three compositions, 73, 75 and 77 at.% Ni, are presented. The interatomic forces are described by Finnis–Sinclair type N-body potentials. The simulations reveal that Ni diffusion is dominated by Ni vacancy mechanisms; Al diffusion is via both the intrasublattice and antistructure bridge (ASB) mechanism in $Ni_{77}Al_{23}$ at the temperatures investigated. The presence of an extra 2% of antisite defects enhances diffusion of both Ni and Al at off-stoichiometric Ni-enriched Ni_3Al via the vacancy–antisite interaction. The single vacancy diffusivity of Ni and Al in Ni_3Al of three compositions, 73, 75 and 77 at.% Ni, at the above temperatures are corrected with thermal equilibrium concentration of point defects. The corrected Ni and Al diffusion data are in good agreement with available experimental data. The Ni diffusivity decreases with the Ni concentration, while Al diffusivity has a minimum at the stoichiometric composition in the simulated temperature range.

1. Introduction

Nickel-aluminides are potential structural materials with applications in high temperature environments. Diffusion is a basic process occurring in creep and phase transformation. Complete understanding of the diffusion mechanisms in nickel-aluminides is of fundamental importance. Despite a great deal of experimental [1–25] and theoretical work [26–32] that has been done on diffusion in stoichiometric Ni_3Al, few relevant results on diffusion in off-stoichiometric Ni_3Al have been reported. Hoshion *et al* [21] showed that the Ni diffusion coefficient is insensitive to the composition change between 24 and 26 at.% Al when the temperature is higher than 1300 K. However, both Hancock *et al* [1] and Shi *et al* [22] showed an increasing trend in D^*_{Ni} with increase in the Ni concentration from 73 to 77 at.% Ni.

Direct measurement of the Al tracer diffusion coefficient in Ni_3Al has been hampered by the lack of a stable ^{26}Al isotope. Ikeda *et al* calculated the Al self-diffusion coefficient D^*_{Al} by fitting the interdiffusion data of a single-phase diffusion couple of Ni_3Al into a Darken–Manning model [23]. The magnitude of D^*_{Al} thus estimated is smaller by a factor of 3–4 at 1400 K than that of D^*_{Ni}. The composition dependence of D^*_{Al} was also examined. D^*_{Al} increases with Al composition, which is consistent with the α-sublattice diffusion mechanism that Al diffuses through the Ni sublattice as an impurity [9]. Recently, Numakura *et al* [24] and Cserháti *et al* [25] reported that the Ni diffusion coefficient is higher than that of Al by an order of magnitude in the stoichiometric composition when temperature is higher than 1400 K.

The role of antisite defects presented in off-stoichiometric positions in diffusion in ordered binary alloys has been studied with Monte Carlo simulations [30–32]. Athénes *et al* modeled diffusion in the $L1_2$ ordered structure of wide composition range ($A_{73}B_{27}$–$A_{77}B_{23}$) [30]. The simulations show that vacancy–antisite interactions contribute to the diffusion of the minority species B; an antisite-assisted sequence also enhances the diffusion of the majority species A in the B-rich composition. The minimum diffusivity of A and B is expected

[1] Present address: Department of Chemistry, Yale University, 225 Prospect Street, New Haven, CT 06520-8107, USA.

 © 2008 IOP Publishing Ltd Printed in the UK

to appear at the stoichiometric composition. Bilova *et al*'s simulations indicate a coupled diffusion effect between Ni and Al diffusion in the presence of antisite defects [31, 32].

To the best of my knowledge there are no comprehensive reports explaining the diffusion mechanisms in $Ni_{77}Al_{23}$ and the composition dependence in Ni_3Al of varying compositions. In previous papers [39, 40], I presented atomistic simulations of Ni, Al diffusion mechanisms in $Ni_{75}Al_{25}$ [39] and $Ni_{73}Al_{27}$ [40]. To complete this series of studies, in this paper I begin by presenting the atomistic simulation results of Ni, Al diffusion mechanisms in $Ni_{77}Al_{23}$. Then I focus on discussing the composition dependence of Ni and Al in Ni_3Al by combining atomistic simulation data obtained in three different compositions, $Ni_{73}Al_{27}$, $Ni_{75}Al_{25}$ and $Ni_{77}Al_{23}$ at the temperature range of 1300–1550 K, with the thermodynamic calculations of the concentration of point defects. I provide the fundamental mechanisms for the composition dependence of Ni and Al diffusion with varying compositions. The rest of the paper is organized as follows. The model and methods applied in this paper are described in section 2. The results and discussion are presented in section 3. The conclusions are summarized in section 4.

2. Model and methods

2.1. Marco-diffusion model

The model describing the diffusion in Ni_3Al at an atomistic level was discussed in detail in the previous papers [1, 2]. In summary, the diffusion process occurring via the vacancy mechanism in Ni_3Al can be described by a vacancy jumping between the nearest lattice sites. In general, jumps can be categorized into either an intrasublattice jump (within the Ni sublattice) or an intersublattice jump (between the Ni sublattice and Al sublattice). To be specific, there are three possible nearest neighbor jumps for either a Ni or Al vacancy, each of which can be defined uniquely with a jump vector. The diffusion mechanisms are identified by analyzing molecular dynamics simulations trajectories. The relative contribution from each diffusion mechanism is quantified with statistics on diffusion events.

In this study, I present a micro-diffusion model for calculating the macro-diffusion coefficients using molecular dynamics simulation data and the equilibrium concentrations of point defects from thermodynamics calculation.

To systematically study the effect of antisite defects on diffusion in γ' Ni_3Al, in all MD simulations the concentration of antisite defects Al_{Ni} and Ni_{Al} in $Ni_{73}Al_{27}$ and $Al_{73}Al_{23}$, respectively, is set to be the equilibrium concentration, while the concentration of the Ni vacancy $C_{V_{Ni}}$ is set to be constant, that is one in 4000 lattices. As analyzed previously [1, 2], the probability of both the Ni and Al intrasublattice jump and intersublattice jump is proportional to the concentration of Ni vacancy and antisite defects.

The simulated self-diffusion coefficient for Ni and Al is fitted to the Arrhenius law [2]

$$D^*_{i_{\rm sim}} = D^0_i \exp\left(\frac{-E^{\rm m}_i}{\kappa_{\rm B} T}\right) \tag{1}$$

where $E^{\rm m}_i$ is the migration energy for Ni or Al atoms in Ni_3Al and $\kappa_{\rm B}$ is the Boltzmann constant.

In order to calculate macroscopic diffusion coefficients, the simulated Ni and Al self-diffusion coefficient, $D^*_{i_{\rm sim}}$, should be corrected with the equilibrium Ni vacancy concentrations. The concentration of antisite point defects $(C_{{\rm Al}_{\rm Ni}}, C_{{\rm Ni}_{\rm Al}})$, which is set to be the equilibrium value, is integrated into the pre-exponential factor in equation (2); whereas the concentration of the Ni vacancy should be corrected with the equilibrium value $C^{\rm eq}_{V_{\rm Ni}}$. Thus, the macro-diffusion coefficient for each atomic species is written as

$$D^*_i = D^*_{i_{\rm sim}} C^{\rm eq}_{V_{\rm Ni}} / C_{V_{\rm Ni}}. \tag{2}$$

The thermal equilibrium concentrations of point defects in Ni_3Al are calculated using the model presented in [37, 38]. There are two constraint conditions in an ordered A_3B crystal having $L1_2$ structure. The first is that the total number of A and B atoms is conserved. The second is the assumption of constancy of stoichiometry, which embodies the identity of the alloy phase even when it is disordered:

$$(n_{{\rm A}\alpha} + n_{{\rm B}\beta})/(n_{{\rm A}\alpha} + n_{{\rm B}\alpha} + n_{{\rm B}\beta} + n_{{\rm A}\beta}) = n_{\rm A}, \tag{3}$$

$$(n_{{\rm A}\alpha} + n^v_\alpha + n_{{\rm A}\beta})/(n_{{\rm B}\beta} + n^v_\beta + n_{{\rm B}\alpha}) = 3, \tag{4}$$

where, n^v_α is the fraction of vacancies on the α sublattice, $n_{\rm A}$ is the number of A atoms and $n_{{\rm A}\beta}$ is the fraction of β sublattice sites occupied by A atoms. The other terms have analogous meanings. In this paper it is assumed that there is no interaction between the point defects in the alloys. Thus, the enthalpy of the alloy with no interacting point defects can be written as

$$\frac{H}{N} = \frac{H_0}{N} + n^v_\alpha H^v_\alpha + n^v_\beta H^v_\beta + n_{{\rm A}\beta} H_{{\rm A}\beta} + n_{{\rm B}\alpha} H_{{\rm B}\alpha}, \tag{5}$$

where N is the total number of atoms in the crystal, H_0 is the enthalpy of the perfect lattice, H^v_α is the vacancy formation enthalpy on the α sublattice in a perfect crystal and $H_{{\rm A}\beta}$ is the formation enthalpy of atom A on the β sublattice in a perfect crystal. The other terms have analogous meanings.

Consider the arrangement of atom A and antisite defects on the α sublattice. Assuming there is no interaction between point defects, the positioning of atom A and antisite defects is random on the α sublattice. The function Ω (the number of microstates) is

$$\Omega = \frac{N_\alpha!}{N_{\rm A}! N_{{\rm B}\alpha}!}, \tag{6}$$

where N_α is the number of α lattice sites, $N_{\rm A}$ is the number of A atoms on the α sublattice and $N_{\alpha B}$ is the number of antisite defects on the α sublattice. The configuration enthalpy of atom A and antisites on the α sublattice is $S = \kappa_{\rm B} \ln(\Omega)$; it will have, using the Stirling approximation,

$$\frac{S}{N} = -\kappa_{\rm B}\left(\frac{N_{{\rm B}\alpha}}{N}\ln\left(\frac{4}{3}\frac{N_{{\rm B}\alpha}}{N}\right) + \frac{N_{\rm A}}{N}\ln\left(\frac{4}{3}\frac{N_{\rm A}}{N}\right)\right) \tag{7}$$

$$= -\frac{3}{4}\kappa_{\rm B}\left(\frac{4}{3}n_{{\rm B}\alpha}\ln\left(\frac{4}{3}n_{{\rm B}\alpha}\right) + \left(1 - \frac{4}{3}n_{{\rm B}\alpha}\right) \times \ln\left(1 - \frac{4}{3}n_{{\rm B}\alpha}\right)\right) \tag{8}$$

$$= -\frac{3}{4}S'\left(\frac{4}{3}n_{{\rm B}\alpha}\right). \tag{9}$$

Equation (9) takes the same form as that of the ideal solid solution, $S' = -\kappa_B(x\ln(x) + (1-x)\ln(1-x))$.

Similarly, the configuration entropy of the vacant sites and atom A on the α sublattice is $\frac{3}{4}S(\frac{4}{3}n_\alpha^v)$. The configuration entropy of the antisite defect and vacant site on the β sublattice is $\frac{1}{4}S(4n_{A\beta})$, and $\frac{1}{4}S(4n_\beta^v)$, respectively. Thus, the total configuration entropy is the summation of the above terms,

$$\frac{S}{N} = \frac{3}{4}\left[S\left(\frac{4n_{B\alpha}}{3}\right) + S\left(\frac{4n_\alpha^v}{3}\right)\right] + \frac{1}{4}\left[S\left(4n_{A\beta}\right) + S\left(4n_\beta^v\right)\right]. \tag{10}$$

If we only consider the vibration entropy (S_{f-A}^v, S_{f-B}^v) introduced by the vacancies:

$$S_f^v = n_\alpha^v S_{f-A}^v + n_\beta^v S_{f-B}^v, \tag{11}$$

the change of the Gibbs free energy of the system is then

$$\Delta G = \Delta H - T\left(S + S_f^v\right). \tag{12}$$

Minimization of the free energy with respect to the concentration of point defects then yields for the vacancy and antisite concentrations,

$$\begin{aligned}
&n_A \geqslant \tfrac{3}{4}\\
&n_\alpha^v = \frac{3}{4}A\left(\frac{4n_{B\alpha}}{1-4n_{B\alpha}}\right)^{n_A-1}\\
&\qquad \times \exp((-H_\alpha^v + (n_A-1)H_{B\alpha})/\kappa_B T)\\
&n_\beta^v = \frac{1}{4}A\left(\frac{4n_{B\alpha}}{1-4n_{B\alpha}}\right)^{n_A}\exp\left((-H_\beta^v + (n_A)H_{B\alpha})/\kappa_B T\right)\\
&n_{A\beta} = \frac{3}{4}A\left(\frac{4n_{B\alpha}}{1-4n_{B\alpha}}\right)^{-1}\exp\left((-H_{A\beta} - H_{B\alpha})/\kappa_B T\right)\\
&n_{B\alpha} = n_{A\beta} + (1-n_A)n_\alpha^v - n_A n_\beta^v + n_A - \tfrac{3}{4}
\end{aligned} \tag{13}$$

$$\begin{aligned}
&n_A \leqslant \tfrac{3}{4}\\
&n_\alpha^v = \frac{3}{4}A\left(\frac{4n_{A\beta}}{1-4n_{A\beta}}\right)^{1-n_A}\\
&\qquad \times \exp((-H_\alpha^v + (1-n_A)H_{A\beta})/\kappa_B T)\\
&n_\beta^v = \frac{1}{4}A\left(\frac{4n_{A\beta}}{1-4n_{A\beta}}\right)^{-n_A}\exp\left((-H_\beta^v - (n_A)H_{A\beta})/\kappa_B T\right)\\
&n_{A\beta} = \frac{3}{4}A\left(\frac{4n_{A\beta}}{1-4n_{A\beta}}\right)^{-1}\exp\left((-H_{A\beta} - H_{B\alpha})/\kappa_B T\right)\\
&n_{A\beta} = n_{B\alpha} + (n_A-1)n_\alpha^v + n_A n_\beta^v - n_A - \tfrac{3}{4}
\end{aligned} \tag{14}$$

where A is defined as $A = e^{S_{f-A}^v/\kappa_B} = e^{S_{f-B}^v/\kappa_B}$. In the present calculation, A is given the value of 4.5, the same as that of pure Ni. The other defect formation enthalpy such as (H_α^v, H_β^v, $H_{A\beta}$, $H_{B\alpha}$) is calculated using the Finnis–Sinclair type of interaction potential [33–36]. The fractional concentration of vacancies and antisite defects is calculated for compositions varying from 72 to 78 at.% Ni for temperatures ranging from 1300 to 1550 K.

The MD simulations begin with the simulation box of 3999 atoms and 1 Ni vacancy. As seen in equation (5), there are no cross terms associated with the bonding energies between point defects. To satisfy this requirement (or to minimize the interaction between point defects), an extra 2% of antisite defects are set on the foreign lattice with the maximum possible separation. During the molecular dynamics simulations, the concentration of point defects reaches dynamic equilibrium, as shown in figure 6 in [39]. The concentration of point defects is small and antisite defects do not segregate in the dynamics simulations. Thus, as long as the initial requirement is met, the simulation results should be reliable. The simulation box containing point defects is artificially increased to the equilibrium volume at the desired temperatures (1300, 1400, 1450, 1500 and 1550 K), heated up and equilibrated. Then the production trajectory of 30 ns typically consisting of 3000 atomic jumps is simulated for each temperature with a timestep of 0.8 fs.

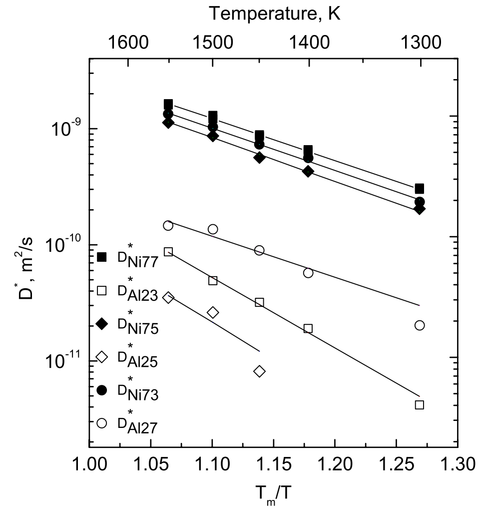

Figure 1. The simulated Ni and Al diffusion coefficient for a single vacancy in γ' Ni_3Al at various temperatures and compositions. The data for $Ni_{75}Al_{25}$ and $Ni_{73}Al_{27}$ are cited from [39] and [40], respectively.

3. Results and discussion

3.1. Temperature dependence of Ni and Al diffusion in $Ni_{77}Al_{23}$

The Ni and Al diffusion coefficients per vacancy in $Ni_{77}Al_{23}$ estimated over the simulated temperature region with equation (1) are pictured in figure 1, where the data for the stoichiometric $Ni_{75}Al_{25}$ [39] and Al-rich $Ni_{73}Al_{27}$ [40] compositions are presented together for comparison. Ni diffusivity per vacancy does not show much temperature dependence between 1300 and 1550 K. It is difficult to observe Al diffusion in $Ni_{75}Al_{25}$ during the 30 ns simulations when the temperature is below 1450 K, as shown in figure 1. In contrast, Al atoms are quite mobile in off-stoichiometric Ni_3Al when the temperature is even lower than 1450 K. It is interesting to note that Ni and Al diffusivity per vacancy in $Ni_{77}Al_{23}$ is higher than that in $Ni_{75}Al_{25}$ by a factor of 1.5 and 2.5, respectively, as depicted in figure 1. To understand the enhanced Ni and Al diffusion in $Ni_{77}Al_{23}$, the diffusion mechanisms for both Ni and Al in $Ni_{77}Al_{23}$ are analyzed in detail in the next section.

Table 1. Statistical results of Ni and Al diffusion in $Ni_{77}Al_{23}$ at different temperatures.

		Ni			Al	
Temp. (K)	N. JMPs	Tot. Ni (%)	Intra. (%)	ASB (%)	Intra. (%)	ASB (%)
1550	5680	88.0	70.0	17.0	23.0	11.6
1500	5147	90.0	71.0	19.0	15.0	17.9
1450	4760	91.0	65.0	24.0	20.0	12.8
1400	4246	94.0	67.0	26.0	26.0	2.2
1300	3754	95.0	54.0	39.0	8.0	—

3.2. Diffusion mechanisms in $Ni_{77}Al_{23}$

3.2.1. Ni diffusion mechanisms in $Ni_{77}Al_{23}$. The molecular dynamics simulation trajectories consisting of a series of elementary jumps were analyzed using a code developed to exhaustively track and sort information pertaining to all possible mechanisms occurring during the dynamics simulations. The data presented in table 1 were calculated as follows. The second column is the total number of atomic jumps at each temperature. The third column shows the number of Ni atom jumps as a percentage of the total atomic jumps. The fourth and fifth column is the number of intrasublattice (Intra.) jumps and antistructure bridge (ASB) mechanism jumps as a percentage of the total Ni atom jumps, respectively. The data for Al atoms (listed in table 1) have an analogous meaning. The number of Al atom jumps as a percentage of the total atomic jumps is not presented for brevity.

As shown in table 1, diffusion of Ni atoms accounts for around 90% of the total number of atomic jumps in $Ni_{77}Al_{23}$ depending on the temperatures simulated. Intrasublattice jumps, in which Ni atoms diffuse through the Ni sublattice, account for 55–70% of the total number of Ni atom jumps, and 17–40% of the total number of Ni atom jumps are ASB jumps in which two successive Ni atom jumps start with an ordering jump ($Ni_{Al} + V_{Ni} \rightarrow V_{Al} + Ni$) followed by a disordering jump ($Ni + V_{Al} \rightarrow Ni_{Al} + V_{Ni}$). It can be concluded that the Intra. and ASB jumps promote Ni atom diffusion in $Ni_{77}Al_{23}$. The contribution of these two mechanisms to Ni diffusion is temperature dependent, i.e. the contribution from the ASB mechanism increases as the temperature decreases.

3.2.2. Al diffusion mechanisms in $Ni_{77}Al_{23}$. The number of Al atom jumps accounts for approximately 5–10% of the total atomic jumps in the simulated temperatures in $Ni_{77}Al_{23}$. Al atoms diffuse by both the Intra. and ASB mechanisms, responsible for 8–26% and 2–18% of total Al atomic jumps, respectively. The Intra. mechanism becomes significantly predominant at lower temperatures ($T < 1400$ K), as shown in table 1. Both the ASB and Intra. mechanisms of Al diffusion are proportional to the concentration of the Ni antisite defects and Ni vacancies. Therefore, it is reasonable to conclude that diffusion of Al atoms is enhanced by the presence of 2 at.% Al antisite defects (Ni_{Al}) given that the concentration of Ni vacancies is fixed in the present simulations.

There is the need to validate the empirical interatomic potentials when they are applied to study diffusion in alloys, as reported in a recent publication [45]. To validate the empirical potential, the simulated results using the empirical potentials are compared with either the *ab initio* calculation results or experimental data. In the case of diffusion at elevated temperatures, it is recommended that experimental data serve as better references for the following reasons. The determination of the diffusion path by *ab initio* calculations of static barriers along a transition path can be incomplete because the diffusion mechanisms in Ni_3Al are temperature dependent, as shown in [39–44]. The molecular dynamics simulation of vacancy diffusion in Ni_3Al using the Finnis–Sinclair type interatomic potential [34] in the present study agree well with the available experimental diffusion data. This suggests that the Finnis–Sinclair type interatomic potential is able to describe the vacancy diffusion mechanisms in Ni_3Al at elevated temperatures. It is worth noting that application of the Finnis–Sinclair type interatomic potential to other diffusion mechanisms in Ni_3Al, such as interstitial diffusion mechanisms, should be done with caution.

3.2.3. Al antisite-assisted diffusion in $Ni_{77}Al_{23}$. One of the primary interests of this paper is focused on the role of the extra 2% of antisite point defects in diffusion in $Ni_{77}Al_{23}$. As mentioned in the previous section, diffusion of Ni and Al atoms in $Ni_{77}Al_{23}$ is faster by a factor of 1.5 and 2.5, respectively, than in $Ni_{75}Al_{25}$. Meanwhile, it is interesting to note that the percentage of ASB jumps of Ni atoms in $Ni_{77}Al_{23}$ is 17–40% of the total Ni atomic jumps compared with 1% in $Ni_{75}Al_{25}$, indicating that the ASB mechanism contributes to the faster Ni diffusion. When Ni atoms perform an ASB jump, a Ni vacancy is transported by one lattice parameter. The link between Ni and Al diffusion can be made through the Ni vacancy, which is actively involved in diffusion of both Ni and Al atoms. Consequently, diffusion of Al atoms in $Ni_{77}Al_{23}$ is enhanced by a factor of 2.5 via the fast transportation of Ni vacancies as a result of the enhanced ASB mechanism for Ni atoms. Belova *et al* [30, 31] reported similar results obtained from Monte Carlo simulation: they found that the diffusion of both components in the ordered compounds of $L1_2$ structure is closely coupled in the presence of a certain number of antisite defects. Athènes *et al* found that in Monte Carlo simulations of diffusion in A_3B binary alloys having $L1_2$ order structure, A diffusion can be enhanced by the presence of A_β antisites [30]. As for the B-rich side, this allows the impurity mechanism to operate and results in enhancement of both A and B diffusion. The molecular dynamics simulation results presented here agree with the results of Athènes [30] and Belova *et al* [31, 32] quantitatively. But here, for the first time, there is a clear picture of the Al–Ni coupled effect in diffusion in Ni-rich off-stoichiometric Ni_3Al at the atomic level. It should be noted that there is no effect of the thermal equilibrium concentration of the Ni vacancy on diffusion in $Ni_{77}Al_{23}$ in the present dynamics simulations. This allows us to focus the effect of an extra 2 at.% of Ni atoms on Ni and Al diffusion in $Ni_{77}Al_{23}$. The Al–Ni coupled effect occurring in the off-stoichiometric Ni_3Al might shed new light on understanding the composition dependence of Ni and Al diffusion in γ' phase Ni_3Al. The temperature and composition

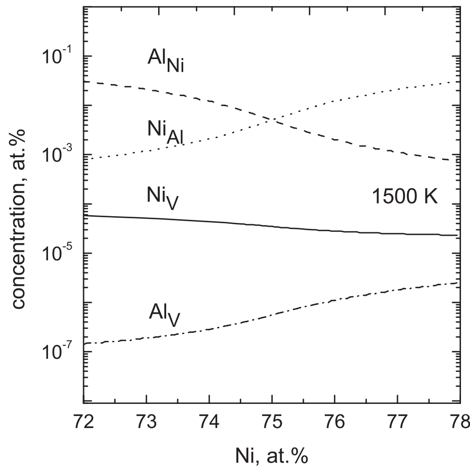

Figure 2. The calculated thermal equilibrium concentration of point defects (Ni_v, Al_v, Ni_{Al}, Al_{Ni}) in γ' Ni_3Al as a function of Ni composition.

dependence of diffusion in Ni_3Al will be discussed in the next section.

3.3. Composition dependence of Ni and Al diffusion in Ni_3Al

To provide insight into the effect of composition on Ni and Al diffusion over a wider composition range, the single vacancy diffusion coefficients for Ni and Al are corrected with the thermal equilibrium concentrations of point defects calculated with the thermodynamic model.

The thermal equilibrium concentrations of point defects in Ni_3Al of 72–78 at.% Ni are calculated in the temperature range between 1300 and 1500 K and the results for 1500 K are presented in figure 2 as an example. The $C_{V_{Ni}}$ concentration decreases with increase in the Ni composition; while the $C_{V_{Al}}$ concentration increases significantly with the Ni composition. At 1500 K, $C_{V_{Ni}}$ in 73 at.% Ni and 77 at.% Ni is higher than that $C_{V_{Al}}$ by two orders and one order of magnitude, respectively.

The corrected diffusion coefficients of Ni and Al obtained via equation (5) as a function of composition at different temperatures are presented in figures 3(a) and (b), respectively. The Ni experimental data obtained by Hoshino *et al* [21] and Shi *et al* [22] are presented in figure 3(a) for comparison. The corrected Ni diffusion coefficients decreases monotonically with increasing Ni composition in the temperature range investigated. The corrected Ni diffusion data agree well with the experimental data in the simulated temperature range. The corrected data predict faster Ni diffusivity for Al-rich Ni_3Al. The results are in accordance with the experimental results of both Hancock *et al* [1] and Shi *et al* [22], although Hoshino *et al* [21] show that the Ni diffusivity is not sensitive to the composition change (73–76 at.% Ni) when the temperature is higher than 1300 K. The trend of variation of the Ni self-diffusion coefficient is the same as that of the Ni vacancy concentration, thus indicating that Ni diffusion in the investigated composition and temperature range is predominantly by the Ni vacancy mechanism. To gain further insight into the problem, a more detailed analysis

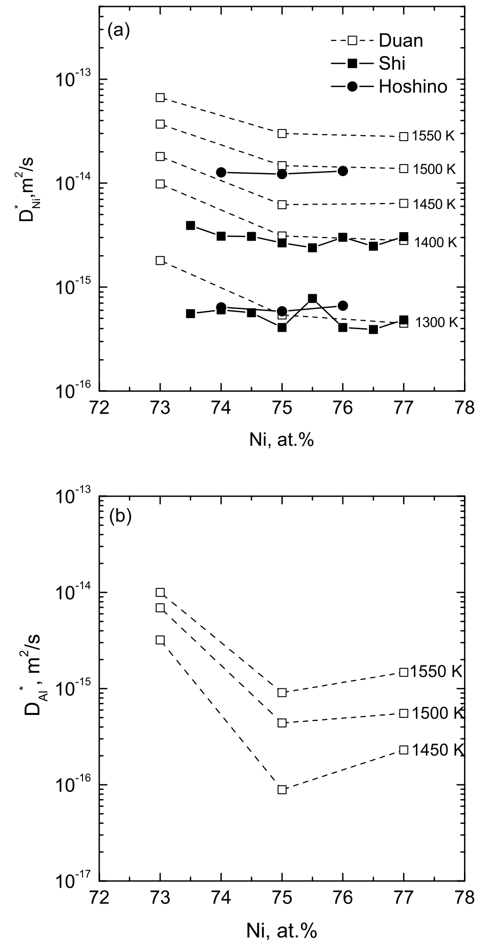

Figure 3. The corrected Ni (a) and Al (b) diffusion coefficients in γ' Ni_3Al as a function of Ni composition. The experimental data for the Ni diffusion coefficient obtained by Hoshino ($T = 1450$, 1300 K) and Shi ($T = 1450$, 1300 K) are presented in (a) for comparison.

is presented as follows. There are two components that are associated with Ni diffusion in off-stoichiometric Ni_3Al: single vacancy diffusivity and the concentration of point defects. The relative contribution of these components is determined by the composition. At a composition of 73 at.% Ni, the Ni diffusivity is enhanced by the fast Ni single vacancy diffusivity and the higher Ni vacancy concentration compared with the stoichiometric composition. At a composition of 77 at.% Ni, the fast Ni single vacancy diffusivity is moderated by the lower Ni vacancy concentration compared with the stoichiometric composition.

The corrected Al simulated data, however, show the composition and temperature dependence, as depicted in figure 3(b). The corrected Al diffusion data in $Ni_{75}Al_{25}$ at 1450 K are of the same order of magnitude as the experimental data ($6 \pm 4 \times 10^{-16}$ m^2 s^{-1}), [25] and theoretical calculation data (8×10^{-16} m^2 s^{-1}) [24]. Due to the Ni vacancy and antisite coupled diffusion effect, as analyzed previously, the minimum Al diffusion coefficient appears at the stoichiometric composition and becomes more distinct as the temperature decreases.

The activation energies for Ni and Al in three compositions are estimated by fitting the corrected Ni and Al

Table 2. The activation energies for Ni and Al diffusion in γ' Ni_3Al of three compositions estimated in this work.

$Ni_{73}Al_{27}$		$Ni_{75}Al_{25}$		$Ni_{77}Al_{23}$	
E_m^{Ni} (eV)	E_m^{Al} (eV)	E_m^{Ni} (eV)	E_m^{Al} (eV)	E_m^{Ni} (eV)	E_m^{Al} (eV)
2.45 ± 0.04	2.15 ± 0.28	2.85 ± 0.10	2.58 ± 0.87	2.77 ± 0.13	2.00 ± 0.11

diffusion coefficients to the Arrhenius law, and are listed in table 2. The activation energies for Ni and Al in $Ni_{75}Al_{25}$ are 2.85 ± 0.10 eV and 2.58 ± 0.87 eV, respectively, which agree well with the experimental values of 3.00 ± 0.10 eV [1] and 2.45 ± 0.15 eV, [29], respectively. There have not been any reports on the activation energies for Al at off-stoichiometric compositions. The quantitatively predicted values from this paper can thus serve as useful references.

The composition dependence of Ni and Al diffusion at lower temperatures is still not clear. Hoshino *et al* [25] and Shi *et al* [26] found that the Ni diffusion coefficient in the same composition region deviates from the Arrhenius law when the temperature is lower than 1273 K. Frank *et al* showed that the straight Arrhenius behavior of Ni diffusion can be extended to as low as 1004 K [7]. They applied highly enriched stable ^{64}Ni as a radiotracer and used secondary ion mass spectrometry to determine the concentration profile. This technique is appropriate for determining slow diffusion at lower temperatures. This result is in agreement with the positron annihilation experiments which indicate that there are no constitutional vacancies in Ni_3Al for all compositions [44]. Further experimental and theoretical research should be performed on the defect structure in γ' Ni_3Al at lower temperatures. Once this information is available, the computational methodology developed in this series of studies (with some necessary modifications) could be used to tackle diffusion mechanisms in γ' Ni_3Al at lower temperatures.

4. Conclusions

Diffusion in $Ni_{77}Al_{23}$ at elevated temperatures (1300–1550 K) is simulated with molecular dynamics using the Finnis–Sinclair interatomic potential. The diffusion mechanisms are revealed and simulated diffusion data are compared with the available experimental data. A thorough understanding of composition dependence of diffusion in Ni_3Al of various compositions is presented. The simulated diffusion data obtained in this study are informative and will motivate further experimental and theoretical investigations. The major conclusions are summarized as follows:

(i) Ni atoms mainly diffuse by the Intra. mechanism in $Ni_{77}Al_{23}$. Al atom diffusion in $Ni_{77}Al_{23}$ is enhanced by the fast migration of Ni vacancies as a result of Intra. and ASB jumps of Ni atoms. The presence of an extra 2 at.% of Ni atoms as antisite defects plays an important role in accelerating Al diffusion.

(ii) Perhaps the most important result reported here is that the thermal equilibrium diffusion coefficients and the migration energies for Ni and Al in Ni_3Al of 73, 75 and 77 at.% Ni have been obtained by correcting atomistic simulation data with the equilibrium concentrations of point defects. For the temperature range simulated, the corrected Ni diffusivity increases with the Al composition; the corrected Al diffusivity is found to be a minimum at the stoichiometric composition. Moreover, the simulations do not merely reproduce the experimental results, they also uncover the underlying mechanisms; in other words, they explain why the experimental results turn out the way they do.

(iii) The diffusion mechanisms and composition dependence of Ni and Al diffusion in Ni_3Al at low temperatures ($T < 1300$ K) are still unknown. More experimental effort is needed to study the defect structure in Ni_3Al at lower temperatures. Looking into the future, the methods developed in these studies of diffusion in γ' Ni_3Al could have important implications for problems that cannot be feasibly studied experimentally, such as Al diffusion in the Ni–Al system over a wide temperature range, and make quantitative predictions for the diffusion data.

References

[1] Hancock G F 1971 *Phys. Status Solidi* a **7** 535

[2] Wang T, Shimotomai M and Doyama M 1984 *J. Phys. F: Met. Phys.* **14** 37

[3] Larikov L N, Grichenko V V and Flachenko V M 1984 *Diffusion Processes in Ordered Alloys* vol 14 (New Delhi: Amerind) (Translated for the Nat. Bur. Standerds and Nat Sci. Found)

[4] Chou T C and Chou Y T 1985 *Mater. Res. Soc. Symp. Proc.* **39** 461

[5] Sitaud B, Zhang X, Dimitrov C and Dimitrov O 1990 *Proc. 1st Eur. Conf.*; *Adv. Mater. Processes* **1** 389

[6] Tarfa T, Dimitrov C and Dimitrov O 1993 *J. Physique* IV **3** 453

[7] Frank S, Söedervall U and Herzig C 1995 *Phys. Status Solidi* b **191** 44

[8] Cermak J and Stloukal I 1997 *Scr. Mater.* **36** 433

[9] Ikeda T, Almazouzi A, Numakura H, Koiwa M, Sprengel W and Nakajima W H 1997 *Defect Diffus. Forum* **143–147** 275

[10] Dimitrov C and Dimitrov O 1997 *Defect Diffus. Forum* **143–147** 215

[11] Frank S, Söedervall U S and Herzig C 1997 *Defect Diffus. Forum* **143–147** 245

[12] Koiwa M, Numakura H and Ishioka S 1997 *Defect Diffus. Forum* **143–147** 209

[13] Badura-Gergen K and Schaefer H-E 1997 *Phys. Rev.* B **56** 3032

[14] Bai B, Fan J and Collins G S 1998 *Mater. Res. Soc. Symp. Proc.* **527** 203

[15] Numakura H, Ikeda T, Nakajima H and Koiwa M 2001 *Defect Diffus. Forum* **194–199** 337

[16] Herzig C, Divinski S V, Frank S and Przeorski T 2001 *Defect Diffus. Forum* **194–199** 317
[17] Numakura H, Ikeda T, Nakajima H and Koiwa M 2001 *Mater. Sci. Eng.* A **A312** 109
[18] Fujiwara K and Horita Z 2002 *Acta Mater.* **50** 1571
[19] Cserhati C, Paul A, Kodentsov A A, van Dal J J H and van Loo F J J 2003 *Intermetallics* **11** 291
[20] Numakura H, Ikeda T, Koiwa M and Almazouzi A 1998 *Phil. Mag.* A **77** 887
[21] Hoshino K, Rothman S J and Averback R S 1988 *Acta Metall.* **36** 1271
[22] Shi Y, Frohberg G and Wever H 1995 *Phys. Status Solidi* a **152** 361
[23] Ikeda T, Almazouzi A, Numakura H, Koiwa M, Sprengel W and Nakajima W H 1998 *Acta Mater.* **46** 5369
[24] Numakura H and Nishi K 2005 *Mater. Sci. Eng.* A **442** 59
[25] Cserháti C, Paul A, Kodentsov A A, van Dal M J H and van Loo F J J 2003 *Intermetallics* **11** 291
[26] Numakura H, Ikeda T, Koiwa M and Almazouzi A 1998 *Phil. Mag.* A **77** 887
[27] Divinski S V, Larikov L V and Shmatko O A 1998 *NATO ASI Series, Series 3: High Technology* vol 59 p 41
[28] Schmidt C and Bocquet J L 1998 *Mater. Res. Soc. Symp. Proc.* **527** 165
[29] Divinski S V, Frank S, Söedervall U and Herzig C 1998 *Acta Mater.* **46** 4369
[30] Athènes M and Bellon P 1999 *Phil. Mag.* A **79** 2243
[31] Belova I V and Murch G E 1998 *Mater. Res. Soc. Symp. Proc.* **527** 159
[32] Belova I V and Murch G E 1999 *Metallofiz. Noveish. Tekhnol.* **21** 36
[33] Finnis M W and Sinclair J E 1984 *Phys. Rev.* B **29** 6443
[34] Vitek V, Ackland G J and Cserti J 1991 *Mater. Res. Soc. Symp. Proc.* **186** 237
[35] Gao F and Bacon D J 1993 *Phil. Mag.* A **67** 275
[36] Gao F and Bacon D J 1993 *Phil. Mag.* A **67** 289
[37] Sun J and Lin D 1994 *Acta Metal. Mater.* **42** 195
[38] Duan J 2002 *PhD Thesis* The University of Liverpool, UK
[39] Duan J 2006 *J. Phys.: Condens. Matter* **18** 1381
[40] Duan J 2007 *J. Phys.: Condens. Matter* **19** 086217
[41] Foiles S and Daw M S 1987 *J. Mater. Res.* **2** 5
[42] Mendelev M I and Bokstein B S 2007 *Mater. Lett.* **61** 2911
[43] Mendelev M I and Ackland G J 2007 *Phil. Mag. Lett.* **87** 349
[44] Mendelev M I, Han S, Son W J, Ackland G J and Srolovitz D J 2007 *Phys. Rev.* B **76** 214105
[45] Meslin E, Fu C C, Barbu A, Gao F and Willaime F 2007 *Phys. Rev.* B **75** 094303